Modelling and Sliding-Mode Control for Launch and Recovery System In Predictable Sea-states with Feasibility Check for Collision Avoidance

Yao Zhang, Christopher Edwards, Michael Belmont and Guang Li

***Abstract*—This paper investigates a deterministic sea wave prediction based non-causal control scheme for the Launch and Recovery from a mother-ship of small rigid-hulled inflatable boats for maritime rescue missions. The proposed control scheme achieves an automatic hoisting process ensuring no collisions occur between the rigid-hulled inflatable boat and mothership hull by using the cable tension force as the manipulated control input. A state-space model of the launch and recovery system is established for the first time where the wave forces and external disturbances such as wind. acting on both the mothership and the small boat are fully considered. A fast and safe recovery is ensured by a fixed-time convergent sliding mode controller, which shortens the cable length to a target value with zero terminal velocity at a pre-defined time instant subject to unknown disturbances and model mismatches. Since the overall dynamics of the swing angle is under-actuated, a feasibility check is proposed to avoid collisions between two vessels and overlarge angular velocities by determining a proper time instant to initiate the hoisting process. To cope with the model mismatch and the external disturbance, the constraints on the swing angle and angular velocity are tightened to ensure safety. The stability of the proposed controller is proven and details of the feasibility check are given. The fidelity of the model and the effectiveness of the proposed scheme is demonstrated in simulation where a realistic sea wave is applied.**

***Index Terms*—Launch and Recovery, Sliding mode control, Deterministic Sea Wave Prediction, Collision avoidance, Tightened constraints, Model mismatch**

I. Introduction

Currently many marine operations, such as Launch and Recovery (L&R) from a mother-ship of small craft, manned and unmanned air vehicles and submersibles, can only be attempted in sufficiently calm sea-states. Although the underlying principles discussed here will be relevant for all these operations, this paper will focus on the recovery of a small manned or unmanned craft. This is typically a rigid-hulled inflatable boat (RHIB). Several marine L&R systems have been investigated, which are the L&R system for autonomous underwater vehicle (UAV) from an unmanned surface vehicle (USV) [1]–[3], the L&R system for helicopter shipboard [4], and the submarine L&R system [5], etc.. In this paper, the recovery operation involves two vessels moving close to each other in proximity (often linked by a bow-line) before the physical connection of the two via a crane/hoist mechanism.

Typically the wave-critical high risk elements of the overall recovery task, i.e. the connection and subsequent hoist of the small craft to the parent vessel, only lasts a few tens of seconds. (Increasing the recovery time increases the operational risk.) In the case where a human initiates recovery, once the two craft are physically connected, the operator is committed to commence the hoisting process. In this context having even short term prediction of quiescent periods of vessel motion, resulting from lower than average wave activity in otherwise large sea states, has considerable operational value. Such fore-knowledge not only increases safety under currently acceptable conditions, but may also allow L&R to be untaken safely in conditions which would at present be deemed un-acceptable.

The relatively recent ability to deterministically predict the evolution of the sea surface over short periods of time [6]–[9] provides such fore-knowledge. This new capability has meant that the use of quiescence prediction in a range of maritime operations is becoming attractive to many modern navies [10]–[12].

In the L&R task, the rescue boat is launched and connected to the mother-ship by a cable, and the hoisting process is achieved by a crane fixed on the mother-ship. The movements of both the mother-ship and the small boat are subject to the wave forces. Once the two craft are physically connected the operator is committed to wait for a proper time instant to initiate the hoisting process. Key constraints applying to the proposed system are as follows. Firstly, collisions between the mother-ship and the small boat should be avoided. Secondly, the terminal cable velocity of the hoist cable should be zero for safety reasons and the hoisting time should be short to ensure fast recovery. Thirdly, overlarge swing angular velocities should be avoided for comfort and safety concerns.

A related class of hoisting problems explored extensively in the literature are the overhead cranes with varying hoist cable length [13]–[15]. Typically, these employ two actuators: one for cargo hoisting and another for trolley driving. In this paper, we consider that there is only one control input which is the tension force along the cable in the L&R system. This restriction increases the difficulty of the controller design, which is further aggravated by the fact that both the crane and the RHIB are subject to relative motion.

Future information of the wave forces acting on both

Y. Zhang is with Department of Mechanical and Construction Engineering, Northumbria University, NE1 8ST, U.K. e-mail: Yao.Zhang@northumbria.ac.uk.

C. Edwards and M. Belmont are with the College of Engineering, Mathematics and Physical Sciences, University of Exeter, Exeter EX4 4QF, U.K. email: C.Edwards@exeter.ac.uk, M.R.Belmont@exeter.ac.uk

G. Li is with School of Engineering and Materials Science, Queen Mary University of London, E1 4NS, U.K. e-mail: g.li@qmul.ac.uk.

This work was supported by EPSRC grant 'Launch and Recovery in Enhanced Sea States' (no. EP/P023002/1).

vessels are assumed to be predicable using the deterministic sea wave prediction (DSWP) technique [16]. This in turn allows the motions of the two crafts, and hence the forces on the L&R system, to be predicted and incorporated into the proposed controller. This results in a non-causal control scheme. Other wave prediction approaches that are based on statistical methods includes auto-regressive prediction models [17], neural network prediction methods [18]. These can be adopted but provide a relatively short period of accurate wave prediction.

To be specific, since the dynamics of the swing angle is under-actuated, the approach to avoid overlarge swing angles and angular velocities during the hoisting process is to initiate the lifting process at a time instant when the 'initial condition' values are sufficiently small. This involves a feasibility check in real time. By checking if the swing angle and the angular velocity at each future steps are within the safety range, one can determine whether the current instant leads to a feasible solution or not. This requires preview information of the future wave forces, which can be provided by DSWP. The L&R task can be divided into two parts. The first part is to determine a proper time instant to initiate the L&R process (by using the preview information of the wave forces from DSWP). Once the L&R process is initiated, the second part is to lift the small boat in two stages.

The challenges of modelling, controller design and feasibility check for the L&R system are as follows:

- Both the varying cable length and the movement of the crane base introduce nonlinearities and varying parameters;
- The coupling between the swing angle dynamics and the cable length dynamics leads to a nonlinear time-varying model of the swing angle dynamics, which increases the difficulty of predicting the swing angle and the angular velocity;
- The external disturbances caused by wind, etc. need to be considered in the modelling and control;
- In the proposed L&R system, only one actuator (producing the tension force along the cable) is considered to guarantee a fast hoisting process without collisions, which is challenging for the controller design.

The contributions and novelties of this paper are as follows:

- A state-space model of the L&R system is developed, where wave forces acting on the vessels and the varying cable length are fully considered;
- A sliding mode controller with pre-defined convergence performance is proposed to steer the cable length and cable velocity to equilibrium points subject to model mismatch;
- A feasibility check method is proposed to detect collisions between the mother-ship and the small boat and any overlarge angular velocities.

The remainder of this paper is organised as follows. In Section II, the three modelling coordinates and the notation are introduced. The state-space model of the L&R system is established by coordinate transformation in Section III, where the hoisting process is divided into two stages. Section IV proposes a fixed-time convergent sliding mode controller, which steers the cable length to the target value with zero terminal velocity during two stages, and the convergence time is proven to be a pre-defined constant. By applying the proposed controller, the predictability of the cable length and cable velocity are guaranteed, which enables the feasibility check method proposed in Section V to avoid collisions and overlarge angular velocities. The simulation results showing the feasibility check and control performance are in Section VI. Section VII concludes this paper.

II. Coordinate and Notation

In this section, the ground coordinates, the mother-ship coordinates and the payload coordinates are introduced. We also introduce the notation and the coordinate transformations employed. A two-dimensional model is considered in this paper partly for the purposes of simplification and partly because the roll motion and the heave motions are related to hull collisions. Yaw and pitch motions projections on the x-o-z coordinate are also included.

A. Coordinates

As shown in Figs. 1(a) and 1(b), three coordinates are introduced in the modelling process: the ground coordinates, the mother-ship coordinates and the payload (small boat) coordinates denoted by $x_0 - O_0 - z_0$, $x_1 - O_1 - z_1$ and $x_2 - O_2 - z_2$, respectively. The details are as follows:

1) $x_0 - O_0 - z_0$: the ground coordinate;
2) $x_1 - O_1 - z_1$: the mother-ship coordinate;
3) $x_2 - O_2 - z_2$: the payload coordinate.

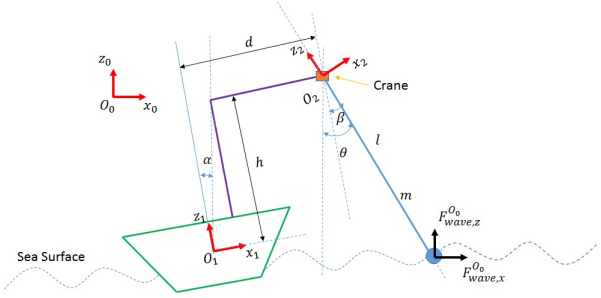

(a) 2D model in Stage 1 (small boat is in the water)

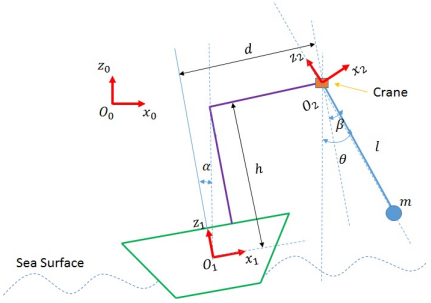

(b) 2D model in Stage 2 (small boat is out of water)

Fig. 1. L&R models in two Stages

The horizontal line towards the right/left of the origin (denoted by O_i) is the positive/negative x_i-axis, and the vertical line

above/below the origin is the positive/negative z_i-axis with $i = 0, 1, 2$. Anticlockwise/clockwise rotation around the origin is positive/negative angle.

B. Notation

TABLE I
NOTATIONS

		Structure parameters
d	$\triangleq$	horizontal distance of crane w.r.t mass centre of mother-ship
h	$\triangleq$	height of crane w.r.t mass centre of mother-ship
		Small boat variables
P^{O_i}	$\triangleq$	position of small boat w.r.t O_i coordinate
V^{O_i}	$\triangleq$	velocity of small boat w.r.t O_i coordinate
A^{O_i}	$\triangleq$	acceleration of small boat w.r.t O_i coordinate
m	$\triangleq$	mass of the small boat
		Angles
α	$\triangleq$	roll angle of the mother-ship w.r.t O_0 coordinate
β	$\triangleq$	swing angle w.r.t O_1 coordinate
θ	$\triangleq$	swing angle w.r.t O_0 coordinate
		mother-ship position
x_m	$\triangleq$	horizontal position of mother-ship w.r.t O_0 coordinate
z_m	$\triangleq$	vertical position of mother-ship w.r.t O_0 coordinate
		State variables
l	$\triangleq$	cable length w.r.t O_0 coordinate
v_L	$\triangleq$	cable velocity w.r.t O_0 coordinate
a_L	$\triangleq$	cable acceleration w.r.t O_0 coordinate
v_θ	$\triangleq$	angular velocity w.r.t O_0 coordinate
		Forces
F^{O_i}	$\triangleq$	Net force acting on the small boat w.r.t O_i coordinate
T	$\triangleq$	Tension force w.r.t O_0 coordinate
$F_{wave,x}/F_{wave,z}$	$\triangleq$	Horizonal/vertical component of wave forces acting on the small boat w.r.t O_0 coordinate
$F_{\epsilon,x}/F_{\epsilon,z}$	$\triangleq$	Horizonal/vertical component of the sum of unknown forces and model mismatch w.r.t O_0 coordinate
g	$\triangleq$	gravitational acceleration w.r.t O_0 coordinate, g = 9.807 m/s^2

C. Coordinate transformation

The coordinates transformation consists of rotational and translational transformations. The rotational transformation is expressed by a rotational matrix $\mathcal{R}(\phi)$ denoting the rotational transformation of two coordinates with ϕ being the angle of rotation from one coordinate frame to the other. As shown in Fig. 2, the $x^{'}$ and $y^{'}$ axes are obtained by rotating the x and y axes counterclockwise through an angle ϕ.

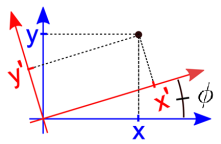

Fig. 2. Rotation of coordinates

Explicitly, the rotation matrix is

$$\mathcal{R}(\phi) := \begin{bmatrix} \cos(\phi) & -\sin(\phi) \\ \sin(\phi) & \cos(\phi) \end{bmatrix} \tag{1}$$

and we have the following relation between two coordinates

$$\begin{bmatrix} x \\ y \end{bmatrix} = \mathcal{R}(\phi) \begin{bmatrix} x^{'} \\ y^{'} \end{bmatrix} \tag{2}$$

Assumption 1. *(Small angle approximation [19]) It is assumed the angle ϕ is sufficiently small such that $\sin(\phi) = \phi$, $\cos(\phi) = 1$ hold. If $\phi \in [-10, 10]$ deg such an assumption holds.*

If the rotation angle satisfies the condition of $\phi \in [-10, 10]$ deg, the derivatives of the rotation matrix are as follows

$$\dot{\mathcal{R}}(\phi) := \begin{bmatrix} -\phi\dot{\phi} & -\dot{\phi} \\ \dot{\phi} & -\phi\dot{\phi} \end{bmatrix} \tag{3}$$

$$\ddot{\mathcal{R}}(\phi) := \begin{bmatrix} -\phi\ddot{\phi} - \dot{\phi}^2 & \phi\dot{\phi}^2 - \ddot{\phi} \\ -\phi\dot{\phi}^2 + \ddot{\phi} & -\phi\ddot{\phi} - \dot{\phi}^2 \end{bmatrix} \tag{4}$$

Using (3) and (4), in the next section, we derive the simplified model of L&R system.

Assumption 2. *The stretch of the cable and the mass of the cable are both negligible.*

Remark 1. *The model mismatch caused by the approximations and assumptions on the cable will be considered in the modelling process and handled by the proposed controller.*

III. Modelling of Launch and Recovery System

In this section, the state-space model for the L&R system is obtained by coordinate transformations. A simplified model is established by using the small angle approximation in Assumption 1. The hoisting process is divided into two stages: when the small boat is in the water and the small boat is out of water. The overall strategy of the proposed scheme is based on the state-space model to be derived as follows.

The position, velocity and acceleration of the small boat w.r.t the payload coordinate O_2 are as follows

$$P^{O_2} = \begin{bmatrix} 0 \\ -l \end{bmatrix}, V^{O_2} = \begin{bmatrix} 0 \\ -\dot{l} \end{bmatrix}, A^{O_2} = \begin{bmatrix} 0 \\ -\ddot{l} \end{bmatrix} \tag{5}$$

By coordinate transformations, the position, velocity and acceleration of the small boat with respect to the ground coordinate $x_0 - O_0 - z_0$ are obtained.

A. Position of the small boat

The position of the small boat can be obtained by transforming from the payload coordinate $x_2 - O_2 - z_2$ to the mother-ship coordinate $x_1 - O_1 - z_1$ and then transforming from the mother-ship coordinate $x_1 - O_1 - z_1$ to the ground coordinate $x_0 - O_0 - z_0$ as follows

1) From O_2 to O_1:

$$P^{O_1} = \mathcal{R}(\beta)P^{O_2} + \begin{bmatrix} d \\ h \end{bmatrix} \tag{6}$$

2) From O_2 to O_0:

$$P^{O_0} = \mathcal{R}(\alpha)P^{O_1} + \begin{bmatrix} x_m \\ z_m \end{bmatrix} \tag{7}$$

$$= \mathcal{R}(\alpha)\mathcal{R}(\beta)P^{O_2} + \mathcal{R}(\alpha)\begin{bmatrix} d \\ h \end{bmatrix} + \begin{bmatrix} x_m \\ z_m \end{bmatrix} \tag{8}$$

$$= \mathcal{R}(\alpha+\beta)P^{O_2} + \mathcal{R}(\alpha)\begin{bmatrix} d \\ h \end{bmatrix} + \begin{bmatrix} x_m \\ z_m \end{bmatrix} \tag{9}$$

B. Velocity of the small boat

The velocity of the small boat can be calculated by taking the first time derivative of P^{O_0} as follows:

$$\begin{aligned} V^{O_0} =& \dot{\mathcal{R}}(\alpha)\mathcal{R}(\beta)P^{O_2} + \mathcal{R}(\alpha)\dot{\mathcal{R}}(\beta)P^{O_2} \\ &+ \mathcal{R}(\alpha)\mathcal{R}(\beta)\dot{P}^{O_2} + \dot{\mathcal{R}}(\alpha)\begin{bmatrix} d \\ h \end{bmatrix} + \begin{bmatrix} \dot{x}_m \\ \dot{z}_m \end{bmatrix} \end{aligned}$$

Considering that $\theta = \alpha + \beta$ holds, we have

$$V^{O_0} = \dot{\mathcal{R}}(\theta)P^{O_2} + \mathcal{R}(\theta)\dot{P}^{O_2} + \dot{\mathcal{R}}(\alpha)\begin{bmatrix} d \\ h \end{bmatrix} + \begin{bmatrix} \dot{x}_m \\ \dot{z}_m \end{bmatrix} \tag{10}$$

C. Acceleration of the small boat

The acceleration of the small boat can be calculated by taking the first time derivative of V^{O_0} as follows:

$$\begin{aligned} A^{O_0} =& \ddot{\mathcal{R}}(\theta)P^{O_2} + 2\dot{\mathcal{R}}(\theta)V^{O_2} \\ &+ \mathcal{R}(\theta)A^{O_2} + \ddot{\mathcal{R}}(\alpha)\begin{bmatrix} d \\ h \end{bmatrix} + \begin{bmatrix} \ddot{x}_m \\ \ddot{z}_m \end{bmatrix} \end{aligned} \tag{11}$$

D. Force

In this subsection, the forces acting on the small boat including the tension force, gravity and predictable wave forces are analyzed. Also, this subsection fully considers uncertainty in the L&R system caused by both external disturbances (such as wind, un-modelled wave forces, etc.) and the modelling approximations (such as modelling assumptions on the cable, etc.)

The launch and recovery process consists of two stages. In Stage 1, the small boat is in the water, and wave forces acting on the small boat should be considered; in Stage 2, the small boat is completely lifted out of water, and the small boat is only subject to the gravity and the tension force along the cable.

Assumption 3. *Assume that the cable is in tension during the whole process.*

The forces acting on the small boat with respect to the ground coordinate can be summarised as

1) Stage 1 (the small boat is in the water):
The force vector acting on the small boat is

$$F^{O_0} = \begin{bmatrix} -T\sin(\theta) + F_{wave,x} + F_{\epsilon,x} \\ T\cos(\theta) - mg + F_{wave,z} + F_{\epsilon,z} \end{bmatrix} \tag{12}$$

2) Stage 2 (the small boat is out of water):
The force vector acting on the small boat is

$$F^{O_0} = \begin{bmatrix} -T\sin(\theta) + F_{\epsilon,x} \\ T\cos(\theta) - mg + F_{\epsilon,z} \end{bmatrix} \tag{13}$$

where $F_{wave,x}$ and $F_{wave,z}$ are x-axis and z-axis components of wave forces, and $F_{\epsilon,x}$ and $F_{\epsilon,z}$ are x-axis and z-axis components of unknown uncertainties, which can be from wind disturbances, etc.

E. Dynamic modelling

Using $F^{O_0} = mA^{O_0}$, we have from (11)

$$\begin{aligned} F^{O_0} =& m\Big(\ddot{\mathcal{R}}(\theta)P^{O_2} + 2\dot{\mathcal{R}}(\theta)V^{O_2} + \\ &\mathcal{R}(\theta)A^{O_2} + \ddot{\mathcal{R}}(\alpha)\begin{bmatrix} d \\ h \end{bmatrix} + \begin{bmatrix} \ddot{x}_m \\ \ddot{z}_m \end{bmatrix}\Big) \end{aligned} \tag{14}$$

The dynamic models of Stage 1 and Stage 2 are as follows

$$\begin{aligned} &\text{Stage 1:} \\ &\begin{bmatrix} -T\sin(\theta) + F_{wave,x} + F_{\epsilon,x} \\ T\cos(\theta) - mg + F_{wave,z} + F_{\epsilon,z} \end{bmatrix} \\ =& m\Big(\ddot{\mathcal{R}}(\theta)P^{O_2} + 2\dot{\mathcal{R}}(\theta)V^{O_2} + \mathcal{R}(\theta)A^{O_2} \\ &+ \ddot{\mathcal{R}}(\alpha)\begin{bmatrix} d \\ h \end{bmatrix} + \begin{bmatrix} \ddot{x}_m \\ \ddot{z}_m \end{bmatrix}\Big) \end{aligned} \tag{15}$$

$$\begin{aligned} &\text{Stage 2:} \\ &\begin{bmatrix} -T\sin(\theta) + F_{\epsilon,x} \\ T\cos(\theta) - mg + F_{\epsilon,z} \end{bmatrix} \\ =& m\Big(\ddot{\mathcal{R}}(\theta)P^{O_2} + 2\dot{\mathcal{R}}(\theta)V^{O_2} + \mathcal{R}(\theta)A^{O_2} \\ &+ \ddot{\mathcal{R}}(\alpha)\begin{bmatrix} d \\ h \end{bmatrix} + \begin{bmatrix} \ddot{x}_m \\ \ddot{z}_m \end{bmatrix}\Big) \end{aligned} \tag{16}$$

Assumption 4. *Both the swing angle θ and the roll angle of the mother-ship α are sufficiently small such that* $\sin(\alpha) = \alpha$, $\cos(\alpha) = 1$, $\sin(\theta) = \theta$ *and* $\cos(\theta) = 1$.

1) Dynamical model of Stage 1: Exploiting Assumption 4, we have the dynamical model of Stage 1 as follows

$$-T\theta/m = \theta\ddot{l} + 2\dot{\theta}\dot{l} + \ddot{\theta}l - \theta\dot{\theta}^2 l + \bar{w}_x - F_{\epsilon,x}/m \tag{17a}$$

$$T/m - g = -\ddot{l} + 2\theta\dot{\theta}\dot{l} + \theta\ddot{\theta}l + \dot{\theta}^2 l + \bar{w}_z - F_{\epsilon,z}/m \tag{17b}$$

where

$$\bar{w}_x = \ddot{x}_m + (-\alpha\ddot{\alpha} - \dot{\alpha}^2)d + (\alpha\dot{\alpha}^2 - \ddot{\alpha})h - F_{wave,x}/m \tag{18}$$

$$\bar{w}_z = \ddot{z}_m + (-\alpha\dot{\alpha}^2 + \ddot{\alpha})d + (-\alpha\ddot{\alpha} - \dot{\alpha}^2)h - F_{wave,z}/m \tag{19}$$

From (17)a $+ \theta \times$ (17)b, we have

$$-g\theta = 2(1+\theta^2)\dot{\theta}\dot{l} + (1+\theta^2)\ddot{\theta}l + \theta\bar{w}_z + \bar{w}_x - \frac{\theta F_{\epsilon,z}}{m} - \frac{F_{\epsilon,x}}{m} \tag{20}$$

and from $-\theta \times (17)\mathrm{a} + (17)\mathrm{b}$, we have

$$\begin{aligned}\frac{T}{m}(1+\theta^2) - g = &-(1+\theta^2)\ddot{l} + (1+\theta^2)\dot{\theta}^2 l \\ &+ \bar{w}_z - \theta\bar{w}_x - \frac{F_{\epsilon,z}}{m} + \frac{\theta F_{\epsilon,x}}{m}\end{aligned} \tag{21}$$

Since θ is small, $1+\theta^2 \approx 1$, (20) and (21) can be simplified to obtain

$$-g\theta = 2\dot{\theta}\dot{l} + \ddot{\theta}l + \theta\bar{w}_z + \bar{w}_x - \frac{\theta F_{\epsilon,z}}{m} - \frac{F_{\epsilon,x}}{m} \tag{22}$$

$$\frac{T}{m} - g = -\ddot{l} + \dot{\theta}^2 l + \bar{w}_z - \theta\bar{w}_x - \frac{F_{\epsilon,z}}{m} + \frac{\theta F_{\epsilon,x}}{m} \tag{23}$$

After simple rearrangements, we have

$$\ddot{\theta} = -\frac{2\dot{\theta}\dot{l}}{l} - \frac{\theta}{l}g - \frac{1}{l}(\theta\bar{w}_z + \bar{w}_x) + \epsilon_\theta \tag{24}$$

$$\ddot{l} = -\frac{T}{m} + g + \dot{\theta}^2 l + (\bar{w}_z - \theta\bar{w}_x) + \epsilon_l \tag{25}$$

where $\epsilon_\theta = \frac{1}{ml}(\theta F_{\epsilon,z} + F_{\epsilon,x})$ and $\epsilon_l = \frac{1}{m}(\theta F_{\epsilon,x} + F_{\epsilon,z})$ are equivalent unknown uncertainties occurring in the θ-dynamics and l-dynamics, respectively.

2) Dynamical model of Stage 2: Following similar reasoning to that used in Stage 1, we obtain

$$\ddot{\theta} = -\frac{2\dot{\theta}\dot{l}}{l} - \frac{\theta}{l}g - \frac{1}{l}(\theta w_z + w_x) + \epsilon_\theta \tag{26}$$

$$\ddot{l} = -\frac{T}{m} + g + \dot{\theta}^2 l + (w_z - \theta w_x) + \epsilon_l \tag{27}$$

where

$$w_x = \ddot{x}_m + (-\alpha\ddot{\alpha} - \dot{\alpha}^2)d + (\alpha\dot{\alpha}^2 - \ddot{\alpha})h \tag{28}$$

and

$$w_z = \ddot{z}_m + (-\alpha\dot{\alpha}^2 + \ddot{\alpha})d + (-\alpha\ddot{\alpha} - \dot{\alpha}^2)h \tag{29}$$

denote the predictable disturbances.

Assumption 5. *The unknown uncertainties in the L&R system are bounded, i.e. there exist positive constants σ_θ and σ_l such that $|\epsilon_\theta| \leq \sigma_\theta$ and $|\epsilon_l| \leq \sigma_l$ hold.*

3) Summary of two dynamical models: Since the dynamical models in two stages are in a similar form, we rewritten the models (24), (25), (26) and (27) as follows

$$\ddot{\theta} = -\frac{2\dot{\theta}\dot{l}}{l} - \frac{\theta}{l}g - \frac{1}{l}D_\theta + \epsilon_\theta \tag{30}$$

$$\ddot{l} = -\frac{T}{m} + g + \dot{\theta}^2 l + D_l + \epsilon_l \tag{31}$$

where

$$D_\theta = \begin{cases}\theta\bar{w}_z + \bar{w}_x, & \text{if} \quad l \geq l_s \\ \theta w_z + w_x, & if \quad l_d \leq l < l_s\end{cases} \tag{32}$$

$$D_l = \begin{cases}\bar{w}_z - \theta\bar{w}_x, & \text{if} \quad l \geq l_s \\ w_z - \theta w_x, & if \quad l_d \leq l < l_s\end{cases} \tag{33}$$

In (32) and (33), l_s is the cable length such that the small boat is just out of water and l_d is the target terminal length of cable. l_s is a time varying variable determined by the predicted wave profile, and l_d is a constant. The values of $\bar{w}_x$, $\bar{w}_z$, w_x and w_z shown in (18), (19), (28) and (29) are assumed to be predicted by the DSWP based on hydrodynamical calculations. In Stage 1, wave forces acting on both the mother-ship and the small boat are considered since the small boat is in the water, and in Stage 2, only the wave force acting on the mother-ship is taken into account since the small boat is out of water. In both stages, the model uncertainties ϵ_θ and ϵ_l are fully considered.

Remark 2. *(Overall strategy) From the cable length dynamics* (31) *and the swing angle dynamics* (30)*, it can be seen that the cable length dynamics is actuated while the swing angle dynamics is under-actuated. Since the swing angle and angular velocity cannot be directly controlled once the hoisting process is initiated, the only way to avoid collisions resulting from overlarge swing angles is to ensure appropriate initial values of the swing angle and angular velocity at the time of initiating hoisting to subsequent future trajectories are within the safe range. Once the predicted trajectories are found to be within the safe range, the corresponding initial time constitutes a proper time instant to initiate the hoisting process.*

The overall strategy for designing the control scheme is as follows:

- *The control input is designed based on the cable length dynamics* (31) *and the feasibility check is designed based on the linked swing angle dynamics* (30)*;*
- *For safety concern, the proposed controller should ensure that the terminal cable velocities at both stages are zero and the convergence time should be short to guarantee a fast lifting process;*
- *To facilitate the feasibility check, the proposed controller should ensure that: 1) the values of the convergence time of both stages are pre-defined constants and independent of wave forces; 2) the cable length and cable velocity at each future step are predictable in order to obtain a prediction model based on* (30)*.*

IV. Fixed-time Convergent Sliding Mode Controller Design

Based on the requirements in Remark 1, a fixed-time convergent sliding mode controller is proposed in this section to: 1) firstly lift the small boat out of water and 2) shorten the length of cable to a desired length with zero terminal velocity, as shown in Fig. 3. For both of these stages, the control objective is to steer the error in cable length (the difference between the target length and the actual length), and the velocity of the cable, to zero, at a specific time instant. Therefore, we propose a fixed-time convergent sliding mode control scheme in Subsection IV-A for Stage 1 and Stage 2, respectively, with the corresponding initial values and desired lengths as described in Subsections IV-B and IV-C. Unlike fixed-time stabilization achieved by using exponential terms [20], [21], this paper designs a time-to-go term to avoid initial overlarge control input that might exceed the actuator limit.

A. Fixed-time Convergent Sliding Mode Control Scheme

Choose the first sliding mode surface as the error in the cable length:

$$s_1 = l - l^* \tag{34}$$

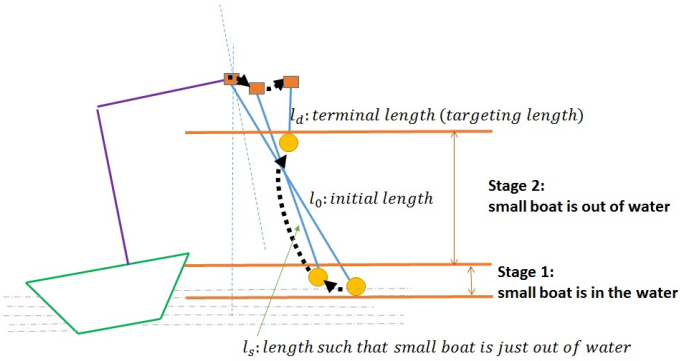

Fig. 3. Whole process of the launch and recovery mission

where l^* is the desired cable length.

Design the reaching law of the first sliding mode, in a time-varying form,

$$\dot{s}_1 = -\frac{k_s}{t_{go}} s_1 \tag{35}$$

where $k_s > 1$ is a positive constant and $t_{go} = t_f - t$ is the time-to-go period for the lifting process, with $t_f > 0$ being a fixed pre chosen terminal time.

Theorem 1. *The sliding surface in* (34) *and its derivative approach zero at $t = t_f$, governed by the reaching law in* (35)*, for any initial values of s_1.*

Proof: Construct a Lyapunov function as

$$V_1 = 0.5 s_1^2 \tag{36}$$

and its time derivative is

$$\dot{V}_1 = s_1 \dot{s}_1 = -\frac{k_s}{t_{go}} s_1^2 < 0, \forall s_1 \neq 0 \tag{37}$$

From (37), global stabilization is proved. Furthermore, during the process as $t \to t_f$, the state s_1 monotonically converges to the origin, and the convergence speed of s_1 increases with t.

Furthermore, to analyze the fixed-time stability, integration of (35) yields

$$s_1(t) = s_{10} \left(\frac{t_{go}}{t_f} \right)^{k_s} \tag{38}$$

where s_{10} is the initial value of $s_1(t)$. Then, its derivative can be obtained as

$$\dot{s}_1(t) = -\frac{k_s}{t_f} s_{10} \left(\frac{t_{go}}{t_f} \right)^{k_s - 1} \tag{39}$$

If we set $k_s - 1$ as a positive constant, both sliding mode surface and its derivative converge to zero as $t \to t_f$ without any information of initial state s_{10}, i.e. $s_1(t) \to 0$, $\dot{s}_1(t) \to 0$ when $t \to t_f$. ■

Since the relationship between position and velocity as shown in (35) is not always satisfied, it is necessary to propose another sliding-mode term to drive the state to the first sliding-mode surface and then keep it staying on the surface.

The following second sliding-mode surface is generated based on the first reaching law in (35):

$$s_2 = \dot{s}_1 + \frac{k_s}{t_{go}} s_1 \tag{40}$$

which means that when $s_2 = 0$ is reached, (35) is automatically satisfied.

The derivative of (40) is given by

$$\dot{s}_2 = \ddot{s}_1 + \frac{k_s}{t_{go}} \dot{s}_1 + \frac{k_s}{t_{go}^2} s_1 \tag{41}$$

Substituting $\ddot{s}_1 = \ddot{l} - \ddot{l}^*$ into (31) yields

$$\ddot{s}_1 = -\frac{T}{m} + g + \dot{\theta}^2 l + D_l + \epsilon_l - \ddot{l}^* \tag{42}$$

Combining (41) and (42) yields

$$\dot{s}_2 = -\frac{T}{m} + g + \dot{\theta}^2 l + D_l + \epsilon_l + \frac{k_s}{t_{go}} \dot{s}_1 + \frac{k_s}{t_{go}^2} s_1 - \ddot{l}^* \tag{43}$$

A control law will now be developed to ensure $s_2 \equiv 0$ in finite time subject to the unknown disturbance ϵ_l.

Theorem 2. *Consider the system in* (30) *and* (31) *with Assumptions 4 and 5 satisfied, then the sliding variable s_2 converges to zero at $t = t_f$ under the proposed controller:*

$$\begin{aligned} T = m(g + \dot{\theta}^2 l + D_l + \frac{k_s}{t_{go}} \dot{s}_1 + \frac{k_s}{t_{go}^2} s_1 + \frac{k_s}{t_{go}} s_2 \\ - \ddot{l}^* + \sigma_l \mathrm{sgn}(s_2)) \end{aligned} \tag{44}$$

for any initial values of s_2, where the function $\mathrm{sgn}(\circ)$ *is defined by* $\mathrm{sgn}(\circ) = \begin{cases} \frac{\circ}{\|\circ\|}, & \circ \neq 0 \\ 0, & \circ = 0 \end{cases}$.

Proof: Consider the following Lyapunov function candidate

$$V_2 = 0.5 s_2^2 \tag{45}$$

and its time derivative

$$\begin{aligned} \dot{V}_2 =& s_2 \dot{s}_2 \\ =& s_2 (-\frac{T}{m} + g + \dot{\theta}^2 l + D_l + \frac{k_s}{t_{go}} \dot{s}_1 + \frac{k_s}{t_{go}^2} s_1 + \epsilon_l - \ddot{l}^*) \end{aligned} \tag{46}$$

Substituting the proposed controller (44) into (46) yields

$$\begin{aligned} \dot{V}_2 &= s_2 \left(-\frac{k_s}{t_{go}} s_2 + \epsilon_l - \sigma_l \mathrm{sgn}(s_2) \right) \\ &\leq -\frac{k_s}{t_{go}} s_2^2 - (\sigma_l - |\epsilon_l|) |s_2| \end{aligned} \tag{47}$$

From (47), since $|\epsilon_l| \leq \sigma_l$ holds, we have $\dot{V}_2 < 0$ for all $V_2 \neq 0$, and $\dot{V}_2 = 0$ holds only when $V_2 = 0$ holds. Furthermore, (47) also gives

$$\dot{V}_2 \leq -\frac{2k_s}{t_{go}} V_2 \tag{48}$$

which yields

$$V_2(t) \leq V_{20} \left(\frac{t_{go}}{t_f} \right)^{2k_s} \tag{49}$$

and

$$\dot{V}_2(t) \leq -\frac{2k_s}{t_f} V_{20} \left(\frac{t_{go}}{t_f}\right)^{2k_s-1} \tag{50}$$

where V_{20} is the initial value of $V_2(t)$.

Since the parameter of the controller is set to be $k_s > 1$, $2k_s - 1$ is a positive constant. Therefore, both the Lyapunov candidate and its derivative converge to zero as $t \to t_f$ regardless of initial state V_{20}. This completes the proof. ■

By substituting (33) into the proposed controller, we have the control input in each stage. The details are in the next two subsections.

B. Controller in Stage 1: the small boat is in the water

In Stage 1, the desired length of cable is such that the small boat is just lifted out of water, i.e. $l^* = l_s$. Substituting $l^* = l_s$ into (34), we have the first sliding surface and reaching law as

$$s_{11} = l - l_s, \dot{s}_{11} = -\frac{k_s}{t_{go}} s_{11} \tag{51}$$

and the second sliding surface as

$$s_{21} = \dot{s}_{11} + \frac{k_s}{t_{go1}} s_{11} \tag{52}$$

where $t_{go1} := t_{f1} - t$ is time-to-go with t_{f1} being the expected convergence time of Stage 1.

Considering (30) $\sim$ (33) and (44), we have the controller in Stage 1 as

$$\begin{aligned} u_1 =& m[g + \dot{\theta}^2 l + (\bar{w}_z - \theta \bar{w}_x) + \frac{k_s}{t_{go1}} \dot{s}_{11} \\ &+ \frac{k_s}{t_{go1}^2} s_{11} + \frac{k_s}{t_{go1}} s_{21} - \ddot{l}_s + \sigma_l \mathrm{sgn}(s_{21})] \end{aligned} \tag{53}$$

C. Controller in Stage 2: the small boat is out of water

In Stage 2, the desired length of cable is a specific value denoted by l_d satisfying $0 < l_d \leq l_s$, i.e. $l^* = l_d$.

The initial values of the cable length, the cable velocity, the swing angle and the angular velocity are given by the terminal values of those in Stage 1. Since $\dot{l}_d = \ddot{l}_d = 0$ holds, by substituting $l^* = l_d$ and $\ddot{l}^* = \ddot{l}_d = 0$ into (34), we have the first sliding surface and reaching law as

$$s_{12} = l - l_d, \dot{s}_{12} = -\frac{k_s}{t_{go}} s_{12} \tag{54}$$

and the second sliding surface as

$$s_{22} = \dot{s}_{12} + \frac{k_s}{t_{go2}} s_{12} \tag{55}$$

where $t_{go2} = t_{f2} - t$ is time-to-go with t_{f2} as the expected convergence time of Stage 2.

Considering (30) $\sim$ (33) and (44), we have the controller in Stage 2 as

$$\begin{aligned} u_2 =& m[g + \dot{\theta}^2 l + (w_z - \theta w_x) + \frac{k_s}{t_{go}} \dot{s}_{12} \\ &+ \frac{k_s}{t_{go2}^2} s_{12} + \frac{k_s}{t_{go2}} s_{22} + \sigma_l \mathrm{sgn}(s_{22})] \end{aligned} \tag{56}$$

V. Feasibility Check For Collision Avoidance

From (30), it can be seen that the swing angle dynamics is under-actuated. Therefore, the only way to ensure the constraints on the swing angle and the angular velocity to be satisfied during the whole process is to ensure appropriate initial values for these two variables, equivalently, a proper initial instant for initiating the hoist.

The feasibility check keeps being repeated at each sampling time. Once the current states are judged to be feasible, i.e. both the swing angle and the angular velocity satisfy the constraints at all future time instants, the launch and recovery process is initiated. Since implementing the online feasibility check in continuous time results in convolution terms that makes the prediction practically intractable, the prediction model is converted to a discrete-time model.

The challenges for the feasibility check come from the nonlinearity and the coupling term in the swing angle dynamics (30), which lead to predictions based on an uncertain model. The details are shown in Subsection V-B. To tackle this issue, this paper takes advantages of the fixed-time convergence property of the controller making the length of cable and the cable velocity at each time instant predictable, and therefore the predictive model of the swing angle dynamics at each step becomes available in advance. In order to tackle the prediction model uncertainty caused by wind, etc., conservatism is built into the feasibility checks via constraint tightening.

A. State-space of the θ-dynamics

Choose the state vector as

$$z = \begin{bmatrix} \theta & v_\theta \end{bmatrix}^{\mathrm{T}} \tag{57}$$

where v_θ is the angular velocity of θ.

The dynamics of the angle in Stage 1 shown in (24) and the dynamics of the angle in Stage 2 shown in (26) can be written as the following state-space forms:

$$\text{Model of Stage } 1 : \dot{z} = A_z z + \bar{D}_z + \Gamma_z \tag{58}$$

and

$$\text{Model of Stage } 2 : \dot{z} = A_z z + D_z + \Gamma_z \tag{59}$$

where

$$\begin{aligned} A_z &= \begin{bmatrix} 0 & 1 \\ -g/l & -2\dot{l}/l \end{bmatrix}, \bar{D}_z = \begin{bmatrix} 0 \\ \frac{\theta}{l}\bar{w}_z + \frac{\bar{w}_x}{l} \end{bmatrix}, \\ D_z &= \begin{bmatrix} 0 \\ \frac{\theta}{l} w_z + \frac{w_x}{l} \end{bmatrix}, \Gamma_z = \begin{bmatrix} 0 \\ \epsilon_\theta \end{bmatrix} \end{aligned}$$

with $\bar{w}_x$ and $\bar{w}_z$ as shown in (18) and (19), and w_x and w_z as shown in (28) and (29).

B. Prediction of Cable Length and Cable Velocity

Note that time-varying variables, the length of cable l, the cable velocity $\dot{l}$ and the swing angle θ, are involved in the matrixes A_z, $\bar{D}_z$ and D_z, which require the future information of the cable length, the cable velocity and the swing angle. Owing to the property of fixed-time convergence arising from the controller designed in the previous section,

future information of the length of cable l and the cable velocity $\dot{l}$ are predictable at each step.

Denote the control steps in the two stages as N_1 and N_2 calculated by $N_1 = t_{f1}/t_s$ and $N_2 = t_{f2}/t_s$, where t_s is the sample time, and N_1 and N_2 are positive integers. N_1 steps of control are used to lift the small boat out of water and another N_2 steps of control are used to complete the remaining task.

Applying the proposed controller (44) to the cable dynamics (31) yields

$$\begin{aligned} a_L(t) \triangleq \ddot{l} = &-\frac{k_s}{t_f - t}\dot{s}_1 - \frac{k_s}{(t_f - t)^2}s_1 - \frac{k_s}{t_f - t}s_2 \\ &+ \ddot{l}^* + \epsilon_l - \sigma_l \mathrm{sgn}(s_2) \end{aligned} \tag{60}$$

Substituting (34) and (40) into (60) and defining $v_s(t) \triangleq \dot{l}_s(t)$, we have

$$\begin{cases} a_L(t) = & -\frac{2k_s}{t_{f1}-t}(v_L(t) - v_s(t)) - \frac{k_s + k_s^2}{(t_{f1}-t)^2}(l(t) - l_s(t)) \\ & +\ddot{l}_s(t) + \Psi(t), 0 \le t < N_1 t_s \\ a_L(t) = & -\frac{2k_s}{t_{f2}-t}v_L(t) - \frac{k_s + k_s^2}{(t_{f2}-t)^2}(l(t) - l_d)red + \Psi(t), \\ & N_1 t_s \le t \le (N_1 + N_2)t_s \end{cases} \tag{61}$$

where $\Psi(t) = \epsilon_l - \sigma_l \mathrm{sgn}(s_2)$, and we have $\|\Psi(t)\| \le 2\sigma_l$.

At each sampling time $t = t_k = kt_s$ with $k = 0, 1, ..., N_1 - 1$, we have

$$\begin{aligned} a_L(t_k) = &-\frac{2k_s}{t_{f1} - t_k}(v_L(t_k) - v_s(t_k)) \\ &- \frac{k_s + k_s^2}{(t_{f1} - t_k)^2}(l(t_k) - l_s(t_k)) + \Psi(t_k) \end{aligned} \tag{62}$$

At each sampling time $t = t_k = kt_s$ with $k = N_1, N_1 + 1, ..., N_1 + N_2 - 1$, we have

$$a_L(t_k) = -\frac{2k_s}{t_{f2} - t_k}v_L(t_k) - \frac{k_s + k_s^2}{(t_{f2} - t_k)^2}(l(t_k) - l_d) + \Psi(t_k) \tag{63}$$

The cable acceleration contains a perturbed part $\Psi(t_k)$ and a nominal part (the first two terms on the right hand sides of (62) and (63)). The nominal part depends on time, the chosen of parameters k_s, t_{f1} and t_{f2} and particular values of $l_s(t_i)$ and $v_s(t_i)$ with $i = 0, 1, ..., N_1 + N_2 - 1$ that can be calculated from the predicted wave profile, and the perturbed part comes from the model uncertainty which is bounded by $\|\Psi(t_k)\| \le 2\sigma_l$. Therefore, the nominal cable length and the nominal cable velocity at each time instant with $i = 0, 1, ..., N_1 + N_2 - 1$ can be calculated by iterations from the nominal parts in (62) and (63) using information of both initial cable length $l(t_0)$ and initial cable velocity $v_L(t_0)$, and the actual cable length $l(t_i)$ and the actual cable velocity $v_L(t_i)$ are their nominal values with bounded errors.

Remark 3. *Owing to the fixed-time convergence property of the proposed controller, the nominal cable length and the nominal cable velocity at each time instant with $i = 0, 1, ..., N_1 + N_2 - 1$ are available in advance. Furthermore, the cable length and cable velocity are independent of the swing angle and angular velocity, which implies that by using the proposed controller, with a specific wave profile, any initial values of swing angle and angular velocity lead to the same variation of nominal cable length and nominal cable velocity. This important property is helpful to identify the time-varying prediction model of the swing angle dynamics, which is used to check the feasibility in the next subsection. These nominal values can be substituted into* (64) *and* (65) *for predicting the future swing angle and future angular velocity. The bounded errors between the nominal values and the actual values of the cable length and the cable velocity further introduce uncertainties to the θ-dynamic prediction model, which is dealt with by constraint tightening in next subsection.*

C. Feasibility check

The whole feasibility check process is shown in Fig. 4. The feasibility check is to ensure the swing angles and angular velocities at each future step are within safety ranges, and this relies on the prediction of the future swing angle and angular velocity before the hoisting process is initiated.

The state-space models of the θ dynamics (58) and (59) are discretized to avoid convolution terms when doing predictions.

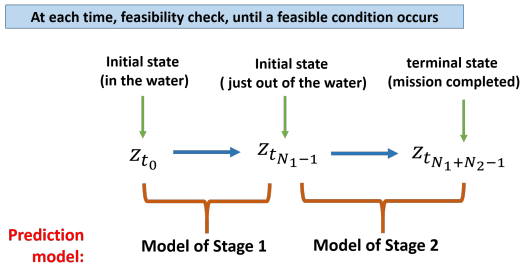

Fig. 4. Diagram of feasibility check procedure

Now two components of uncertainty are present in the prediction process. One is the model uncertainty denoted by Γ_z in the θ-dynamics model (58) and (59), and the other is from the bounded error between the nominal values and the actual values of the cable length and the cable velocity, as mentioned in Remark 3. These two elements of uncertainties are lumped into one term denoted by $\Delta(k)$ and incorporated into the prediction model as follows

$$\text{Model of Stage 1}: z_{k+1} = A_{zk}(k)z_k + \bar{D}_k(k) + \Delta(k) \tag{64}$$

$$\text{Model of Stage 2}: z_{k+1} = A_{zk}(k)z_k + D_k(k) + \Delta(k) \tag{65}$$

where

$$A_{zk}(k) = \begin{bmatrix} 1 & t_s \\ -\frac{gt_s}{\bar{l}(t_k)} & 1 - \frac{2\bar{v}_L(t_k)t_s}{\bar{l}(t_k)} \end{bmatrix},$$

$$\bar{D}_k(k) = \begin{bmatrix} 0 \\ \frac{\theta(t_k)}{\bar{l}(t_k)}\bar{w}_z(t_k)t_s + \frac{\bar{w}_x(t_k)}{\bar{l}(t_k)}t_s \end{bmatrix},$$

$$D_k(k) = \begin{bmatrix} 0 \\ \frac{\theta(t_k)}{\bar{l}(t_k)}w_z(t_k)t_s + \frac{w_x(t_k)}{\bar{l}(t_k)}t_s \end{bmatrix}$$

where $\bar{l}(t_k)$ and $\bar{v}_L(t_k)$ denote the nominal cable length and the nominal cable velocity, respectively.

To rule out the possibility of collisions arising from the unknown model uncertainties $\Delta(k)$, we tighten the constraints on the swing angle and angular velocity. The main idea is to make sure '*the worst case*' is coped with, by using the upper bound of the model uncertainties to obtain a conservative solution.

Assumption 6. *The model uncertainty $\Delta(t_k)$ is bounded by a constant vector, i.e. $\Delta(t_k) \in \mathbb{W}_\Delta$, and $\mathbb{W}_\Delta := \{-\Delta_{max} \preceq \Delta(t_k) \preceq \Delta_{max}\}$ with $\Delta_{max} \in \mathbb{R}^2$ a positive constant vector.*

By assuming all the state variables keep constant during each sampling interval and considering the model uncertainty caused by the discretization, we have the following discrete-time model:

The prediction model can be obtained by rewriting (64) and (65) as follows

$$\begin{aligned}\begin{bmatrix}\theta(t_{k+1})\\ v_\theta(t_{k+1})\end{bmatrix} =&\bar{A}_\theta(t_k)\begin{bmatrix}\theta(t_k)\\ v_\theta(t_k)\end{bmatrix} + \bar{\Phi}_\theta(t_k) + \Delta(t_k),\\ &k = 0, 1, ..., N_1 - 1\end{aligned} \tag{66}$$

$$\begin{aligned}\begin{bmatrix}\theta(t_{k+1})\\ v_\theta(t_{k+1})\end{bmatrix} =&A_\theta(t_k)\begin{bmatrix}\theta(t_k)\\ v_\theta(t_k)\end{bmatrix} + \Phi_\theta(t_k) + \Delta(t_k),\\ &k = N_1, N_1+1, ..., N_1+N_2-1\end{aligned} \tag{67}$$

where

$$\begin{aligned}\bar{A}_\theta(t_k) &= \begin{bmatrix}1 & t_s\\ -\frac{gt_s}{\bar{l}(t_k)} + \frac{\bar{w}_z(t_k)t_s}{\bar{l}(t_k)} & 1 - \frac{2\bar{v}_L(t_k)t_s}{\bar{l}(t_k)}\end{bmatrix},\\ A_\theta(t_k) &= \begin{bmatrix}1 & t_s\\ -\frac{gt_s}{\bar{l}(t_k)} + \frac{w_z(t_k)t_s}{\bar{l}(t_k)} & 1 - \frac{2\bar{v}_L(t_k)t_s}{\bar{l}(t_k)}\end{bmatrix},\\ \bar{\Phi}_\theta(t_k) &= \begin{bmatrix}0\\ \frac{\bar{w}_x(t_k)t_s}{\bar{l}(t_k)}\end{bmatrix}, \Phi_\theta(t_k) = \begin{bmatrix}0\\ \frac{w_x(t_k)t_s}{\bar{l}(t_k)}\end{bmatrix}\end{aligned} \tag{68}$$

Remark 4. *Note that future information regarding the nominal cable lengths $\bar{l}(t_k)$ and nominal cable velocities $\bar{v}_L(t_k)$ with $k = 0, ..., N_1 + N_2 - 1$ can be calculated from future information of $\bar{w}_x(t_k)$ and $\bar{w}_z(t_k)$ with $k = 0, ..., N_1 - 1$ and that future information of $w_x(t_k)$ and $w_z(t_k)$ with $k = N_1, ..., N_1 + N_2 - 1$ are available from the DSWP. Therefore, the prediction models* (66) *and* (67) *are perturbed models with known nominal parts and bounded additive disturbances. Since the additive disturbance is bounded by a known constant vector by Assumption 6, the most conservative way to avoid constraint violations can be obtained by 1) considering the worst case where the disturbance amplitude is assumed to be its maximum Δ_{max} at every future step; 2) and tightening the constraint based to this worst case.*

The future N_1-step-ahead predictions of the swing angle and the angular velocity can be written as

$$\begin{bmatrix}z(t_1)\\ z(t_2)\\ z(t_3)\\ \vdots\\ z(t_{N_1})\end{bmatrix} = \bar{F}z(t_0) + \bar{G}\begin{bmatrix}\bar{\Phi}_\theta(t_0) + \Delta(t_0)\\ \bar{\Phi}_\theta(t_1) + \Delta(t_1)\\ \bar{\Phi}_\theta(t_2) + \Delta(t_2)\\ \vdots\\ \bar{\Phi}_\theta(t_{N_1-1}) + \Delta(t_{N_1-1})\end{bmatrix} \tag{69}$$

where

$$\bar{F} = \begin{bmatrix}\bar{A}_\theta(t_0)\\ \bar{A}_\theta(t_0)\bar{A}_\theta(t_1)\\ \bar{A}_\theta(t_0)\bar{A}_\theta(t_1)\bar{A}_\theta(t_2)\\ \vdots\\ \bar{A}_\theta(t_0)\cdots\bar{A}_\theta(t_{N_1-1})\end{bmatrix},$$

$$\bar{G} = \begin{bmatrix}I_2 & 0 & 0 & \cdots & 0\\ \bar{A}_\theta(t_1) & I_2 & 0 & \cdots & 0\\ \bar{A}_\theta(t_1)\bar{A}_\theta(t_2) & \bar{A}_\theta(t_2) & I_2 & \cdots & 0\\ \vdots & \vdots & \vdots & \ddots & \vdots\\ \bar{g}_1 & \bar{g}_2 & \bar{g}_3 & \cdots & I_2\end{bmatrix},$$

$$\begin{aligned}\bar{g}_1 &= \bar{A}_\theta(t_1)\cdots\bar{A}_\theta(t_{N_1-1}),\\ \bar{g}_2 &= \bar{A}_\theta(t_2)\cdots\bar{A}_\theta(t_{N_1-1}),\\ \bar{g}_3 &= \bar{A}_\theta(t_3)\cdots\bar{A}_\theta(t_{N_1-1}).\end{aligned}$$

The further N_2-step-ahead predictions of the swing angle and the angular velocity can be written as

$$\begin{bmatrix}z(t_{N_1+1})\\ z(t_{N_1+2})\\ z(t_{N_1+3})\\ \vdots\\ z(t_{N_1+N_2})\end{bmatrix} = Fz(t_{N_1}) + G\begin{bmatrix}\Phi_\theta(t_{N_1}) + \Delta(t_{N_1})\\ \Phi_\theta(t_{N_1+1}) + \Delta(t_{N_1+1})\\ \Phi_\theta(t_{N_1+2}) + \Delta(t_{N_1+2})\\ \vdots\\ \Phi_\theta(t_{N_1+N_2-1}) + \Delta(t_{N_1+N_2-1})\end{bmatrix} \tag{70}$$

where

$$F = \begin{bmatrix}A_\theta(t_{N_1})\\ A_\theta(t_{N_1})A_\theta(t_{N_1+1})\\ A_\theta(t_{N_1})A_\theta(t_{N_1+1})A_\theta(t_{N_1+2})\\ \vdots\\ A_\theta(t_{N_1})\cdots A_\theta(t_{N_1+N_2-1})\end{bmatrix},$$

$$G = \begin{bmatrix}I_2 & 0 & 0 & \cdots & 0\\ A_\theta(t_{N_1+1}) & I_2 & 0 & \cdots & 0\\ A_\theta(t_{N_1+1})A_\theta(t_{N_1+2}) & A_\theta(t_{N_1+2}) & I_2 & \cdots & 0\\ \vdots & \vdots & \vdots & \ddots & \vdots\\ g_1 & g_2 & g_3 & \cdots & I_2\end{bmatrix},$$

$$\begin{aligned}g_1 &= A_\theta(t_{N_1+1})\cdots A_\theta(t_{N_1+N_2-1}),\\ g_2 &= A_\theta(t_{N_1+2})\cdots A_\theta(t_{N_1+N_2-1}),\\ g_3 &= A_\theta(t_{N_1+3})\cdots A_\theta(t_{N_1+N_2-1}).\end{aligned}$$

Define the safety ranges of angle and angular velocity as $\Omega_\theta = \{\theta|\theta \in [\theta^{min}, \theta^{max}]\}$ and $\Omega_{v\theta} = \{v_\theta \in [v_\theta^{min}, v_\theta^{max}]\}$ with $\theta^{min} < \theta^{max}$ and $v_\theta^{min} < v_\theta^{max}$.

Define constraint vectors as $z_{min} = [\theta^{min}, v_\theta^{min}]^{\mathrm{T}}$ and $z_{max} = [\theta^{max}, v_\theta^{max}]^{\mathrm{T}}$.

Given the current swing angle and angular velocity $z(t_0)$, the feasibility check is to check if all the future states $z(t_i)$ with $i = 1, ..., N_1+N_2-1$ are within the constraint as follows

$$z_{min} \preceq z(t_i) \preceq z_{max} \tag{71}$$

which is equivalently to check the following two inequalities

$$\begin{bmatrix} z_{min} \\ z_{min} \\ z_{min} \\ \vdots \\ z_{min} \end{bmatrix} + \bar{G} \begin{bmatrix} \Delta_{max} \\ \Delta_{max} \\ \Delta_{max} \\ \vdots \\ \Delta_{max} \end{bmatrix} \preceq \bar{F} z(t_0) + \bar{G} \begin{bmatrix} \bar{\Phi}_\theta(t_0) \\ \bar{\Phi}_\theta(t_1) \\ \bar{\Phi}_\theta(t_2) \\ \vdots \\ \bar{\Phi}_\theta(t_{N_1-1}) \end{bmatrix} \preceq \begin{bmatrix} z_{max} \\ z_{max} \\ z_{max} \\ \vdots \\ z_{max} \end{bmatrix} - \bar{G} \begin{bmatrix} \Delta_{max} \\ \Delta_{max} \\ \Delta_{max} \\ \vdots \\ \Delta_{max} \end{bmatrix} \tag{72}$$

$$\begin{bmatrix} z_{min} \\ z_{min} \\ z_{min} \\ \vdots \\ z_{min} \end{bmatrix} + \bar{G} \begin{bmatrix} \Delta_{max} \\ \Delta_{max} \\ \Delta_{max} \\ \vdots \\ \Delta_{max} \end{bmatrix} \preceq F z(t_{N_1}) + G \begin{bmatrix} \Phi_\theta(t_{N_1}) \\ \Phi_\theta(t_{N_1+1}) \\ \Phi_\theta(t_{N_1+2}) \\ \vdots \\ \Phi_\theta(t_{N_1+N_2-1}) \end{bmatrix} \preceq \begin{bmatrix} z_{max} \\ z_{max} \\ z_{max} \\ \vdots \\ z_{max} \end{bmatrix} - \bar{G} \begin{bmatrix} \Delta_{max} \\ \Delta_{max} \\ \Delta_{max} \\ \vdots \\ \Delta_{max} \end{bmatrix} \tag{73}$$

VI. Numerical Simulation

A realistic sea wave heave trajectory gathered from the coast of Cornwall, UK is used to test the control performance of the proposed scheme (shown in Fig. 5). The wave forces acting on the mothership and the small boat are generated by the hydrodynamic software WAMIT [22].

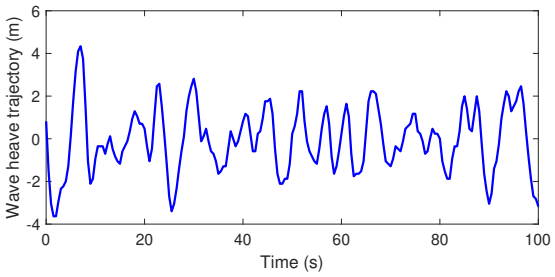

Fig. 5. A realistic sea wave heave trajectory gathered from the coast of Cornwall, UK

A type of commercial RHIB developed by a British company Ribcraft [23] is used as the small boat to be hoisted (Dry weight: 275 kg, maximum load capacity: 765 kg). In what follows assume the total mass of the small boat is at its maximum value $m = 275 + 765 = 1040$ kg. The initial length of cable is $l(t_0) = 6$ m, initial cable velocity is $v(t_0) = 0$ m/s. The parameter of the controller is $k_s = 2$ in (53) and (56), which satisfies the condition of fixed-time stabilization as discussed in Section IV-A. The safety regions of the swing angle and angular velocity are $\Omega_\theta = \{\theta | \theta \in [-10 \text{ deg}, 10 \text{ deg}]\}$ and $\Omega_{v\theta} = \{v_\theta | v_\theta \in [-10 \text{ deg/s}, 10 \text{ deg/s}]\}$.

Model uncertainties arising from modelling errors, prediction errors and wind, etc. is considered in the following form

$$\begin{aligned} \epsilon_\theta(t) &= \epsilon_\theta(t_0) e^{\lambda_1 t} + \xi_1(t) \\ \epsilon_l(t) &= \epsilon_l(t_0) e^{\lambda_2 t} + \xi_2(t) \end{aligned} \tag{74}$$

where $\lambda_1 > 0$ and $\lambda_2 > 0$ have been chosen to match with realistic model uncertainties including prediction errors that grows with the prediction time. $\xi_1(t), \xi_2(t) \sim \mathcal{N}(0, 0.2)$, $\epsilon_\theta(t_0) \sim \mathcal{N}(0, 2)$ and $\epsilon_\theta(t_0) \sim \mathcal{N}(0, 1)$ are Gaussian white noises.

Based on the test environment above, the simulation is divided into four parts as follows:

- Model fidelity: The differences between the response of the original model and the simplified model based on Assumption 2 are quantified to demonstrate the model fidelity.
- Feasibility check: Determine a proper time t_0 to initiate the L&R process that ensures both the swing angle and the angular velocity are within the safety range.
- Control performance: In Stage 1, lift the small boat out of water in 1.5 sec with zero terminal cable velocity relative to the surface of the water. In Stage 2: Lift the small boat up to a specific height $l_d = 3.5$ m in 1 sec with zero terminal cable velocity. The model uncertainty is given by (74).
- Monte Carlo simulation for robustness validation: To demonstrate the robustness of the proposed controller, a set of Monte Carlo simulation with 100 cases with initial perturbations and model uncertainties listed in Table II is undertaken.

TABLE II
Model Uncertainties And Initial Perturbations

Parameters	Mean value	Standard dev.
Small boat mass m	1040 kg	50 kg
Initial cable length l_0	6 m	0.5 m
Initial cable velocity v_{L0}	0 m/s	0.5 m/s
Model uncertainty parameter λ_1	0.3	0.1
Model uncertainty parameter λ_2	0.3	0.1

A. Fidelity validation of the simplified model

The simplified model described in (30) and (31) is based on Assumption 4. As shown in Fig. 6, to quantify the affect of this assumption on the model fidelity, the root mean squared errors (RMSEs) of the swing angle θ and the angular velocity v_θ between the original model and the simplified model are employed, which are calculated by

$$RMSE(\theta) = \left(\frac{1}{n} \sum [\theta(k) - \bar{\theta}(k)]^2 \right)^{1/2}$$

and

$$RMSE(v_\theta) = \left(\frac{1}{n} \sum [v_\theta(k) - \bar{v}_\theta(k)]^2 \right)^{1/2}$$

where $\theta(k)$ and $\bar{\theta}(k)$ denote the k-th sampled swing angles of the original model and the simplified model respectively, and $v_\theta(k)$ and $\bar{v}_\theta(k)$ denote the k-th sampled angular velocities of the original model and the simplified model respectively, and

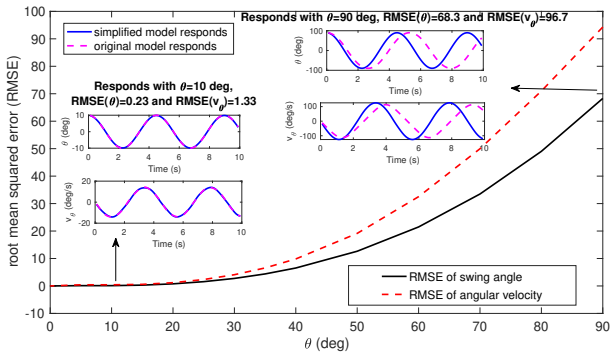

Fig. 6. RMSE vs Swing angle θ

n is the number of samples. It can be found that the simplified model used to design the controller and check the feasibility is of high fidelity for swing angles within the safety region $\Omega_\theta = \{\theta|\theta \in [-10 \text{ deg}, 10 \text{ deg}]\}$.

B. Feasibility check

In this subsection, the proposed feasibility check is applied to a realistic situation where a wave gathered from the coast of Cornwall is used. The incoming wave information is assumed to be available by DSWP. The model uncertainty is considered as in (74). The predictable terms w_x, w_z, $\bar{w}_x$ and $\bar{w}_z$ generated from the wave profile are shown in Fig. 7.

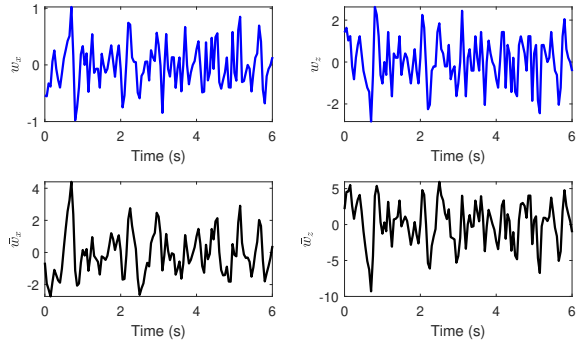

Fig. 7. w_x, w_z, $\bar{w}_x$ and $\bar{w}_z$ generated from a realistic wave

With this wave profile and a particular set of initial swing angles and angular velocities, $\theta(t_0) = 5$ deg and $v_\theta(t_0) = 0$ deg/s, at each sampling time, the feasibility check is employed to determine whether the current instant is an appropriate initial time that ensures no collisions and no overlarge angular velocities. The feasibility check is shown in Fig. 8. Since the model mismatch caused by wind, currents etc. is considered as in (74), the constraints on both swing angle and angular velocity are tightened from the original region ($\Omega_\theta = \{\theta|\theta \in [-10 \text{ deg}, 10 \text{ deg}]\}$ and $\Omega_{v\theta} = \{v_\theta|v_\theta \in [-10 \text{ deg/s}, 10 \text{ deg/s}]\}$) to a tightened one ($\Omega_\theta = \{\theta|\theta \in [-8.1 \text{ deg}, 8.1 \text{ deg}]\}$ and $\Omega_{v\theta} = \{v_\theta|v_\theta \in [-7.7 \text{ deg/s}, 7.7 \text{ deg/s}]\}$) in order to rule out the possibilities of constraint violation caused by model mismatch (see the blue dashed lines in Fig. 8). The feasible solution is found and the corresponding initial time is determined as $t = 2.5$ s (see red lines in Fig. 8).

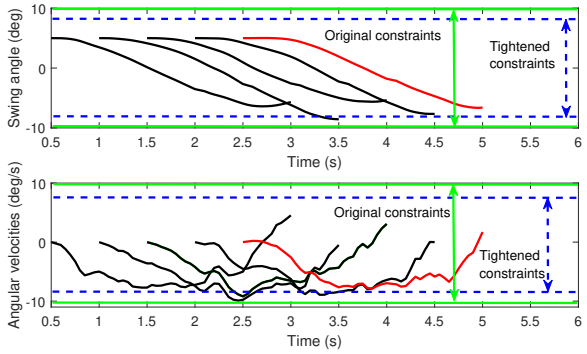

Fig. 8. Predicted trajectories with different wave profiles. (Red line: feasible trajectories, Black line: non-feasible trajectories, Green line: Original constraints, Blue line: Tightened constraints)

C. Control performance

From the feasible solution found by the feasibility check (red lines in Fig. 8), the initial time to start the L&R is $t = 2.5$s, and the initial swing angle and angular velocity are $[\theta(t_0), v_\theta(t_0)] = [5 \text{ deg}, 0 \text{ deg/s}]$. In this subsection, the corresponding actual trajectories of the states and tension force obtained by using the proposed controller are shown. Three cases are tested to demonstrate the effectiveness of the proposed SMC.

- Case 1: An ideal situation where no disturbances are present, and σ_l is set to zero in the controller (44);
- Case 2: The disturbances modelled by (74) are included, and $\sigma_l = 4$ is chosen as the bound of equivalent disturbance acceleration;
- Case 3: The disturbances modelled by (74) are included, but σ_l is set to zero in the controller (44).

The simulation results of the control performance for these three cases are shown in Figs. 9 $\sim$ 11.

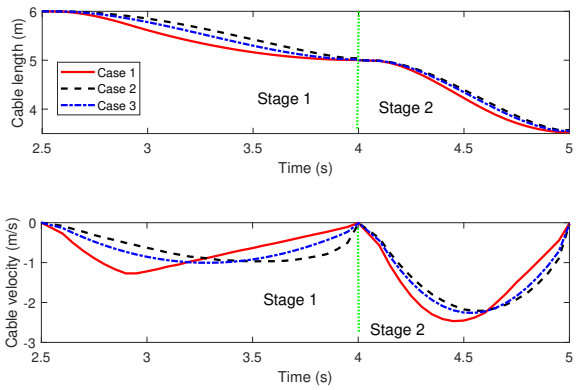

Fig. 9. Trajectories of cable lengths and velocities in three cases

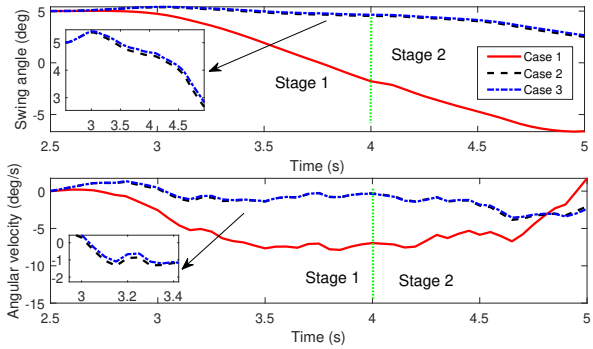

Fig. 10. Trajectories of swing angles and angular velocities in three cases

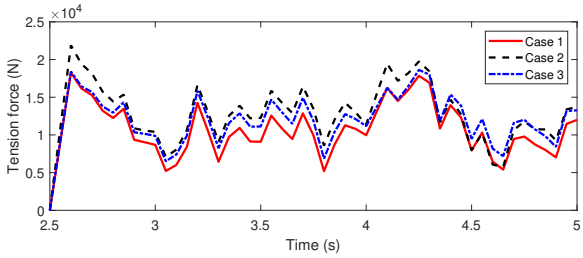

Fig. 11. Trajectories of tension forces in three cases

From Fig. 9, it can be seen that the proposed controller ensures that the cable length can be shortened to a target value with zero terminal relative velocity with and without disturbances. The convergence time of the two stages is verified to be the pre-defined values. From the comparison between Case 1 and Case 2 in Fig. 10, it can be seen that the swing angle and angular velocity are significantly affected by the model mismatch and the disturbance but are still within the constraints, which verifies the effectiveness of feasibility check and the controller. From the comparison between Case 2 and Case 3 in Figs. 9 and 10, it can be seen that the cable length and the cable velocity are changed by the switching term σ_l in the controller when disturbances are present, whilst the swing angle and the angular velocity are barely affected. From Fig. 11, the tension force required to complete the L&R subject to unknown disturbances is within 25000 N, which is acceptable for Marine L&R operations.

D. Monte Carlo simulation for robustness validation

In this subsection, 100 cases with initial perturbations and model uncertainties listed in Table II are tested to demonstrate the robustness of the proposed controller. From Fig. 12, it can be seen that with model uncertainties and initial perturbations, the proposed controller successfully completes the L&R process with all the trajectories converging to desired values. This demonstrates the robustness of the proposed controller against unknown disturbances. It can be seen from Fig. 13 that swing angles and angular velocities with different initial values and model uncertainties are all within safety ranges. This verifies that the possibility of collisions and overlarge angular velocities is ruled out even though the model uncertainty is taken into account.

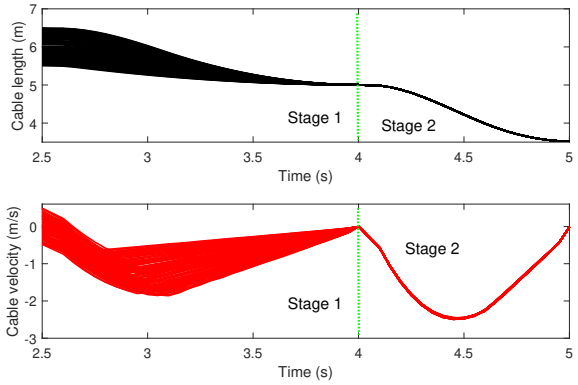

Fig. 12. 100 trajectories of cable length and velocity with model uncertainty and initial perturbations

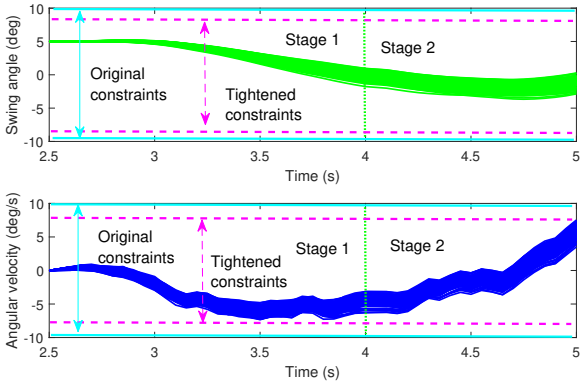

Fig. 13. 100 trajectories of swing angle and angular velocity with model uncertainty and initial perturbations

TABLE III
STEADY-STATE ERROR FROM MONTE CARLO RESULTS

Parameters	Average value	Maximal value
Cable length in Stage 1	0.043 m	0.082
Cable velocity in Stage 1	0.031 m/s	0.04 m/s
Cable length in Stage 2	0.028 m	0.05 m
Cable velocity in Stage 2	0.3 m/s	0.07 m/s

The steady-state errors of cable length and cable velocity in Stage 1 and Stage 2 are summarised in Table III, from which it can be found that the maximal steady-state errors by using the proposed controller are 0.082 m (approximately 1.6% of desired value) and 0.07 m/s. Therefore, the robustness of the proposed controller is verified.

VII. CONCLUSIONS

This paper has proposed a state-space model of a Launch and Recovery system, which considers the wave forces acting on the mother-ship and the small boat and the external disturbance caused by wind and currents. The hoisting process consists of two stages: the stage when the small boat is in the water and the stage when the small boat is out of water. Based on the wave prediction method, a feasibility

check was13 designed to determine a proper time instant to initiate the hoisting process. A fixed-time convergent sliding mode controller was proposed to shorten the cable length to the target value with zero relative terminal velocity subject to unknown disturbances. To consider other challenging control problems related to the launch and recovery system, future work will focus on a three-dimensional modelling with detailed mechanisms, including the crane motor driving mechanism, cable damping mechanism, and proper controllers applying to the three-dimensional model.

REFERENCES

[1] EI Sarda and MR Dhanak. A usv-based automated launch and recovery system for auvs. *IEEE journal of oceanic engineering*, 42(1):37–55, 2016.

[2] EI Sarda and MR Dhanak. Launch and recovery of an auv from a station-keeping usv.

[3] EI Sarda. *Automated Launch and Recovery of an Autonomous Underwater Vehicle from an Unmanned Surface Vessel*. Florida Atlantic University, 2016.

[4] DY Lee, N Sezer-Uzol, JF Horn, and LN Long. Simulation of helicopter shipboard launch and recovery with time-accurate airwakes. *Journal of Aircraft*, 42(2):448–461, 2005.

[5] HL Zhang, ZY Deng, and YG Luo. Development actuality of submarine launch and recovery system. *Ship Science and Technology*, 34(4):3–6, 2012.

[6] M Al-Ani, J Christmas, MR Belmont, JM Duncan, J Duncan, and B Ferrier. Deterministic sea waves prediction using mixed space–time wave radar data. *Journal of Atmospheric and Oceanic Technology*, 36(5):833–842, 2019.

[7] MR Belmont, J Christmas, J Dannenberg, T Hilmer, J Duncan, JM Duncan, and B Ferrier. An examination of the feasibility of linear deterministic sea wave prediction in multidirectional seas using wave profiling radar: Theory, simulation, and sea trials. *Journal of Atmospheric and Oceanic Technology*, 31(7):1601–1614, 2014.

[8] T Hilmer and E Thornhill. Deterministic wave predictions from the wamos ii. In *OCEANS 2014-TAIPEI*, pages 1–8. IEEE, 2014.

[9] E Blondel, G Ducrozet, F Bonnefoy, and P Ferrant. Deterministic reconstruction and prediction of non-linear wave systems. *Proc. of the 23rd Int. Work. on Water Waves and Floating Bodies*, 2008.

[10] P Crossland, B Ferrier, and J Duncan. The feasibility of developing a quiescent period prediction system in a simulation environment. In *RINA International Conference on Computer Applications in Shipbuilding ICCAS 2009*, 2009.

[11] JM Giron-Sierra and S Esteban. The problem of quiescent period prediction for ships: A review. *IFAC Proceedings Volumes*, 43(20):307–312, 2010.

[12] B Ferrier, J Duncan, MR Belmont, A Curnow, P Crossland, and J Duncan. Using simulation to justify and develop quiescent period prediction systems for the royal navy. In *Royal Institution of Naval Architects-International Conference on Computer Applications in Shipbuilding*, volume 2, pages 99–107, 2013.

[13] AT Le, A Janchiv, GH Kim, and SG Lee. Feedback linearization control of overhead cranes with varying cable length. *International Journal of Precision Engineering and Manufacturing*, 13(4):501–507, 2012.

[14] AT Le, SC Moon, WG Lee, and SG Lee. Adaptive sliding mode control of overhead cranes with varying cable length. *Journal of Mechanical Science and Technology*, 27(3):885–893, 2013.

[15] Y Wu, N Sun, H Chen, J Zhang, and Y Fang. Nonlinear time-optimal trajectory planning for varying-rope-length overhead cranes. *Assembly Automation*, 38(5):587–594, 2018.

[16] MR Belmont, JMK Horwood, RWF Thurley, and J Baker. Filters for linear sea-wave prediction. *Ocean Engineering*, 33(17-18):2332–2351, 2006.

[17] Francesco Fusco and John V Ringwood. Short-term wave forecasting for real-time control of wave energy converters. *IEEE Transactions on sustainable energy*, 1(2):99–106, 2010.

[18] MC Deo and C Sridhar Naidu. Real time wave forecasting using neural networks. *Ocean engineering*, 26(3):191–203, 1998.

[19] ML Boas. *Mathematical methods in the physical sciences*. John Wiley & Sons, 2006.

[20] Andrey Polyakov. Nonlinear feedback design for fixed-time stabilization of linear control systems. *IEEE Transactions on Automatic Control*, 57(8):2106–2110, 2011.

[21] Wei He, Fengshou Kang, Linghuan Kong, Yanghe Feng, Guangquan Cheng, and Changyin Sun. Vibration control of a constrained two-link flexible robotic manipulator with fixed-time convergence. *IEEE Transactions on Cybernetics*, 2021.

[22] Massachusetts Institute of Technology. https://www.wamit.com.

[23] British Ribcraft company. https://www.ribcraft.co.uk/rescue-ribs/.

Yao Zhang (M'20) received her Ph. D. in Department of Control Science and Engineering, specialized in control systems and deep space explorations, from Harbin Institute of Technology, in 2018. She is currently a senior lecturer in Department of Mechanical and Construction Engineering, University of Northumbria, Newcastle upon Tyne, U.K. Her research interest covers sliding mode control, model predictive control and control applications, etc. She is an Associate Editor of IET Generation, Transmission, and Distribution.

Christopher Edwards is a Professor of control engineering with the College of Engineering, Mathematics and Physical Sciences, University of Exeter, U.K. He is a co-author of 400 refereed papers in his areas of interest and of three books: Sliding Mode Control: Theory and Applications (Taylor & Francis, 1998), Fault Detection and Fault Tolerant Control using Sliding Modes (Springer-Verlag, 2011), and Sliding Mode Control and Observation (Birkhauser, 2013). In addition, he recently coedited the monograph Fault Tolerant Flight Control: A Benchmark Challenge (Springer-Verlag, 2010). His current research interests include sliding-mode control and observation and their application to fault detection and fault-tolerant control. Dr. Edwards is currently Chair of the IEEE Technical Committee on Variable Structure Systems.

Michael Belmont is currently a Professor of marine dynamics at the University of Exeter, Exeter, U.K., where he is responsible for maritime systems research. The main application of his present research is in enhancing the wave limits under which marine operations can be safely conducted. Underpinning this work are the new subjects of deterministic sea wave prediction and the intimately linked field of Quiescent Period Prediction, both of which he pioneered.

Guang Li received the Ph.D. degree in electrical and electronics engineering, specialized in control systems from the University of Manchester, Manchester, U.K., in 2007. He is currently a Reader of dynamics modeling and control with the Queen Mary University of London, London, U.K. His current research interests include constrained optimal control, model predictive control, adaptive robust control, and control applications, including renewable energies and energy storage.